Pollen Tube Growth Oscillations and Intracellular Calcium Levels Are Reversibly Modulated by Actin Polymerization[1]

Luis Cárdenas*, Alenka Lovy-Wheeler, Joseph G. Kunkel, and Peter K. Hepler

Departamento de Biología Molecular de Plantas Instituto de Biotecnología, Universidad Nacional Autónoma de México, Cuernavaca, Morelos 62271, Mexico (L.C.); Department of Biology and the Plant Biology Graduate Program, University of Massachusetts, Amherst, Massachusetts 01003 (J.G.K., P.K.H.); and Department of Neuroscience, Tufts School of Medicine, Boston, Massachusetts (A.L.-W.)

Prevention of actin polymerization with low concentrations of latrunculin B (Lat-B; 2 nM) exerts a profound inhibitory effect on pollen tube growth. Using flow-through chambers, we show that growth retardation starts after 10 min treatment with 2 nM Lat-B, and by 15 to 20 min reaches a basal rate of 0.1 to 0.2 μm/s, during which the pollen tube exhibits relatively few oscillations. If treated for 30 min, complete stoppage of growth can occur. Studies on the intracellular Ca^{2+} concentration indicate that the tip-focused gradient declines in parallel with the inhibition of growth. Tubes exhibiting nonoscillating growth display a similarly reduced and nonoscillating Ca^{2+} gradient. Studies on the pH gradient indicate that Lat-B eliminates the acidic domain at the extreme apex, and causes the alkaline band to move more closely to the tip. Removing Lat-B and returning the cells to control medium reverses these effects. Phalloidin staining of F-actin reveals that 2 nM Lat-B degrades the cortical fringe; it also disorganizes the microfilaments in the shank causing the longitudinally oriented elements to be disposed in swirls. Cytoplasmic streaming continues under these conditions, however the clear zone is obliterated with all organelles moving into and through the extreme apex of the tube. We suggest that actin polymerization promotes pollen tube growth through extension of the cortical actin fringe, which serves as a track to target cell wall vesicles to preferred exocytotic sites on the plasma membrane.

Actin plays a central role in the control of pollen tube growth (Hepler et al., 2001). It is well appreciated that acto-myosin drives cytoplasmic streaming, including the transport of the secretory vesicles that are essential for the apical extension of this rapidly growing cell. More recently we have come to realize that actin polymerization also participates in the pollen tube growth process (Gibbon et al., 1999; Vidali et al., 2001; Cárdenas et al., 2005; Chen et al., 2007). Either preventing (Gibbon et al., 1999; Vidali et al., 2001; Chen et al., 2007) or enhancing (Cárdenas et al., 2005) polymerization profoundly affects pollen tube growth. The studies with agents that block polymerization have been especially insightful. Thus the injection of excess profilin or DNase, or the treatment of cells with cytochalasin D (CD) or latrunculin B (Lat-B) all cause a reduction in the growth rate at substantially lower concentrations than needed to inhibit cytoplasmic streaming (Vidali et al., 2001). Vidali et al. (2001) further found that 1 nM Lat-B, over time, caused a marked reduction in growth in which the oscillations in growth rate were damped or possibly even eliminated. These results support the idea that actin polymerization is necessary for pollen tube growth.

Together with these physiological data have been recent structural observations that help us appreciate where and how actin is involved in apical growth. Recent studies from Lovy-Wheeler et al. (2005) show that pollen tubes of lily (*Lilium* spp.) and tobacco (*Nicotiana tabacum*) possess a striking cortical fringe of F-actin in the apical domain. In lily pollen tubes, this actin fringe starts a few microns back from the tip and extends basally for an additional 5 to 10 μm. Historically we note that this fringe, although observed on few previous occasions, has been difficult to preserve, probably owing to its fragility. It seems likely that the cortical actin fringe is the key structure that undergoes rapid remodeling and polymerization, which then plays a central role in pollen tube growth.

Attempts to monitor the activity of apical actin have met with considerable difficulty; nevertheless two reports have addressed this issue in pollen tubes exhibiting oscillatory growth. Fu et al. (2001), using Arabidopsis (*Arabidopsis thaliana*) pollen expressing GFP-talin, report that the amount of F-actin, identified as short actin bundles, increases in the apex in antici-

[1] This work was supported by the National Science Foundation, (grant nos. MCB–0077599 and MCB–0516852 to P.K.H.). This work was also supported by grants from Dirección General de Asuntos del Personal Académico de la Universidad Nacional Autónoma de México (grant nos. IN228903 and IN206507 to L.C.).

* Corresponding author; e-mail luisc@ibt.unam.mx.

The author responsible for distribution of materials integral to the findings presented in this article in accordance with the policy described in the Instructions for Authors (www.plantphysiol.org) is: luisc@ibt.unam.mx (luisc@ibt.unam.mx)

[OA] Open Access articles can be viewed online without a subscription.

www.plantphysiol.org/cgi/doi/10.1104/pp.107.113035

pation of an increase in the growth rate. More recently Lovy-Wheeler et al. (2007) followed the actin-dependent motion of the endoplasmic reticulum (ER), and found that it exhibited an oscillatory character, in which it moved forward, forming a platform structure, in advance of the increase in growth rate. As a leader, actin structure and activity might be part of the mechanism that initiates the surge in growth.

If actin polymerization and activity are growth-initiating processes, what then regulates actin? Some obvious candidates include actin binding proteins (e.g. profilin, gelsolin/villin, and actin depolymerizing factor [ADF]), perhaps especially in response to certain regulatory ions (e.g. Ca^{2+} and H^{+}). Briefly we note that all these components are well represented in the apex of growing pollen tubes (Hepler et al., 2001). Calcium (Ca^{2+}) and pH gradients are well expressed, and exhibit oscillations (Hepler et al., 2006). Of particular note, recent work reveals that an increase in the alkaline band, which resides in the clear zone near the cortical actin fringe, occurs in anticipation of an increase in growth (Lovy-Wheeler et al., 2006). In addition, ADF and actin interacting protein, which form a pH sensitive actin binding protein complex, colocalize with the actin fringe. It is plausible that the rise in pH in the alkaline band stimulates ADF, which through fragmentation of existing F-actin, exposes new plus ends and promotes polymerization of new microfilaments (Lovy-Wheeler et al., 2006). Ca^{2+} can also be expected to regulate the actin cytoskeleton. In the region of the tip-focused Ca^{2+} gradient it is reasonable to predict that gelsolin/villin would fragment existing F-actin (Fan et al., 2004; Huang et al., 2004; Yokota and Shimmen, 2006; Xiang et al., 2007), and that profilin would retard polymerization of new microfilaments (Kovar et al., 2000). However, the oscillatory increase in Ca^{2+} follows, rather than leads, growth (Messerli et al., 2000), causing us to suggest that this ion together with its associated actin binding protein acts as a growth retarder, not promoter. At the same time we must keep in mind that actin itself might serve as a regulator of ions; studies, including one on pollen grain protoplasts and pollen tubes (Wang et al., 2004), report that actin regulates Ca^{2+}.

With these questions in mind we have revisited the role of actin polymerization in the control of pollen tube growth. Herein we examine the effect of low concentrations of Lat-B on pollen tube growth, and also on intracellular Ca^{2+} and pH. Lat-B (2 nM) has a profound but selective effect on the actin cytoskeleton; it destroys the cortical actin fringe but retains arrays, albeit disorganized, of microfilaments in the shank of the tube. Using a flow through culture chamber, where changes in growth rate and ions can be followed with great care, we find that 2 nM Lat-B markedly slows cell elongation, leading to a situation in which basal growth occurs, but oscillatory growth is eliminated. Under these circumstances the tip-focused Ca^{2+} gradient declines and the alkaline band moves closer to the apex. These results enhance our understanding of the role of actin polymerization in pollen tube growth.

RESULTS

Actin Polymerization Is Necessary for Oscillatory Pollen Tube Growth

When 2 nM Lat-B is administered to pollen tubes exhibiting oscillatory growth, there is no apparent effect for the first 5 min (Fig. 1A). However, during the next 10 to 15 min the overall growth rate starts to decline; the oscillations become erratic with a marked diminution in excursions from the midpoint to high growth rates. During the next 20 min the growth rate declines further with the pollen tube exhibiting mainly a basal rate of growth with a few brief excursions to the formerly midlevel rate of growth (Fig. 1, A and B). This condition of basal, nonoscillating growth can be sustained for 10 min; if the pollen tube is retained in 2 nM Lat-B, cell extension will eventually stop completely after 30 min (Fig. 1B). Of particular note, these effects are completely reversible when the pollen tube is returned to normal, control conditions. Following removal of Lat-B, the tubes require a few minutes (approximately 5 min) to reinitiate growth (Fig. 1B). At first there are fluctuations between nongrowth and a basal rate, but after 10 min, the tube typically exhibits a basal, nonoscillating rate of growth. After 20 min, oscillations to higher values of growth become evident and within 30 min the tube exhibits normal oscillatory growth, which is equivalent to that seen prior to Lat-B treatment (Fig. 1B). A summary shown in Figure 1C emphasizes the reversibility of the Lat-B effect, where the expressions of normal growth, slow growth, and a return to normal growth are visually juxtaposed.

Lat-B Profoundly Affects the Cortical Actin Fringe

To monitor the effect of Lat-B on the structure of the actin cytoskeleton, we have fixed pollen tubes according to the room temperature protocol developed recently by Lovy-Wheeler et al. (2005). This procedure, which uses glutaraldehyde together with ethylene glycol bis[sulfosuccinimidylsuccinate], a protein cross-linking reagent that effectively stabilizes actin microfilaments, reveals a prominent cortical fringe of actin in the apical domain of the pollen tube (Fig. 2A; Lovy-Wheeler et al., 2005). The fringe starts about 3 μm behind the tip and extends basally for another 7 μm. In the shank, basal to the fringe, the microfilaments are also longitudinally oriented but more evenly dispersed throughout the tube. Treatment with 2 nM Lat-B (Fig. 2, B and C) causes a marked degradation of the cortical fringe. However, the microfilaments in the shank are still present, although their pattern is disrupted, wherein the relatively straight and longitudinally oriented elements become disorganized into swirls.

Lat-B (2 nM) Causes a Decline in the Tip-Focused Ca^{2+} Gradient

Treatment of pollen tubes with 2 nM Lat-B, which degrades the cortical fringe and slows growth, also

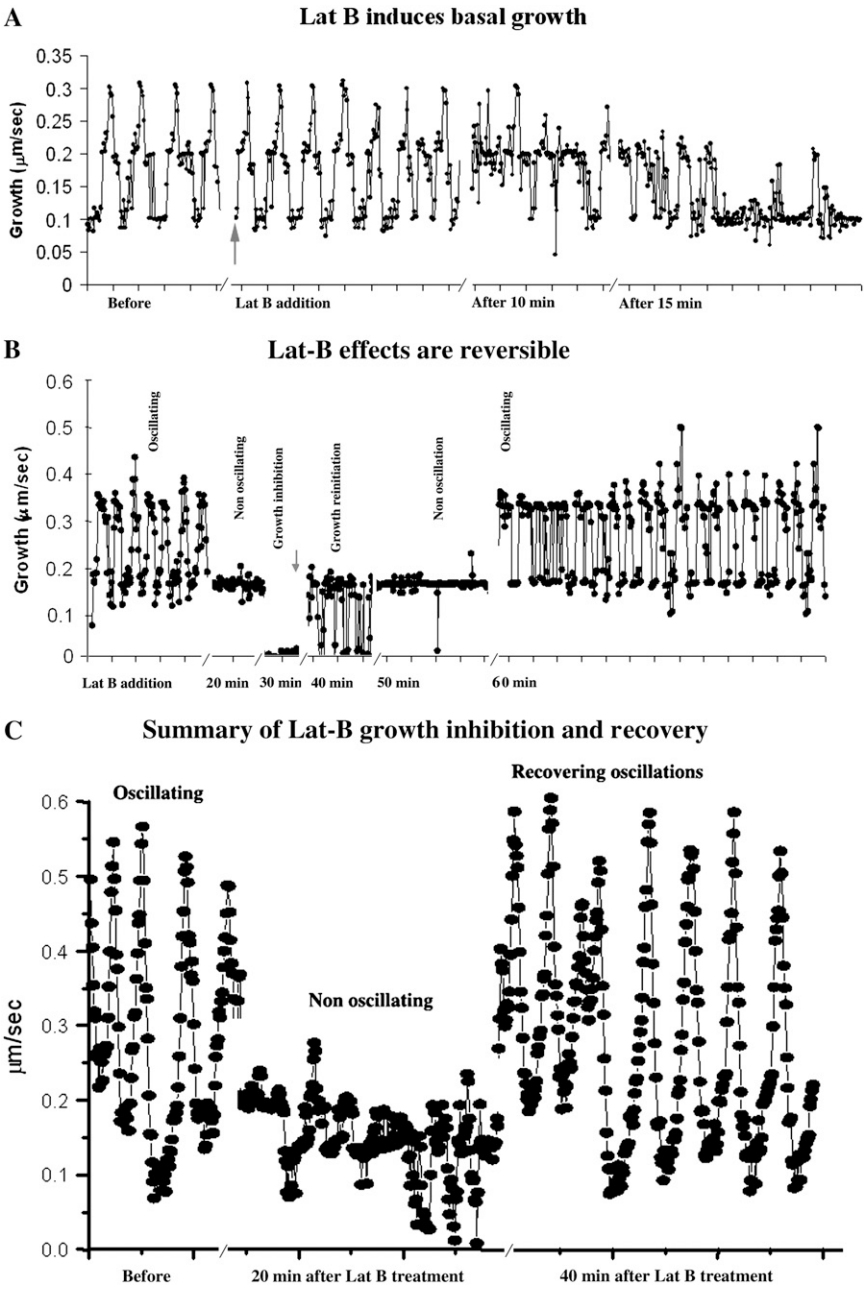

Figure 1. Graphs showing the changes in pollen tube growth rate in response to application of Lat-B (2 nM). These data, which are representative of 10 different cells, show individual pollen tubes that have been cultured in microscope chambers in which the medium composition has been controlled by a flow-through pump. Figure 1A shows details on the initial effects of Lat-B on the growth rate. No effect is observed during the first 5 min. After 10 min the growth rate starts to decline, and by 20 min approaches a basal, nonoscillating condition. Figure 1B shows growth inhibition and recovery in response to Lat-B addition and removal. After 30 min in Lat-B, growth is fully inhibited. Nevertheless, when Lat-B is removed, full recovery of oscillatory growth occurs over the next 30 to 40 min. Figure 1C provides a summary of normal growth, nonoscillating growth and full recovery.

profoundly affects the tip-focused Ca^{2+} gradient (Fig. 3). In close agreement with the growth data, 5-min treatment causes only a slight lowering of the Ca^{2+} gradient (Fig. 3B), whereas by 15 min it is much more pronounced (Fig. 3C). Whenever pollen tubes exhibit basal growth, there is always an accompanying gradient even though it may only be 500 nM at the high point. However, if pollen tube growth is completely inhibited, then the Ca^{2+} gradient declines to basal values of 100 to 200 nM, which are expressed throughout the length of the tube (Fig. 3D). As with the growth data, even when the Ca^{2+} gradient is totally eliminated, it can recover when the pollen tube is returned to control culture medium (Fig. 3E).

The detailed relationship between Ca^{2+} and growth oscillations in pollen tubes treated with Lat-B is shown in Figure 4. Under control conditions Ca^{2+} and growth oscillate with the same period, but not exactly with the same phase. As previously shown by Messerli et al. (2000) and repeated here, when these two sets of oscillatory data are subjected to cross-correlation analysis, the Ca^{2+} pulse follows the increase in growth rate by approximately 1 to 4 s, or 15° to 60° (Fig. 4A). Ca^{2+} changes therefore appear to be dependent on the preceding growth pulse, rather than growth being dependent on Ca^{2+}. By monitoring growth and Ca^{2+} in cells cultured in a flow through chamber we see that after 15 min in Lat-B they both decline in parallel (Fig. 4, B

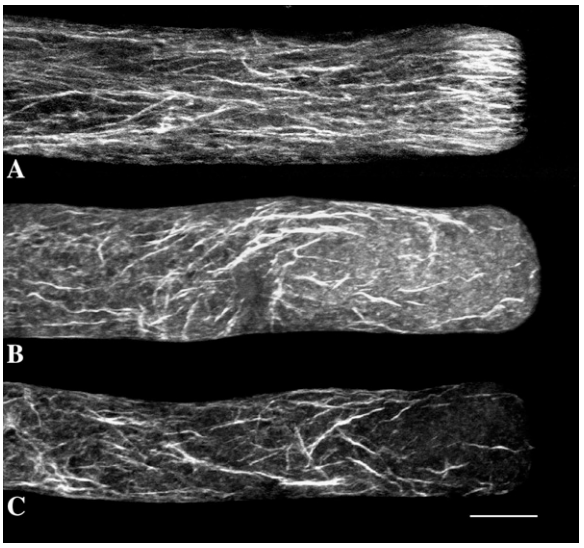

Figure 2. Effect of Lat-B on F-actin: Figure 2A shows the actin cytoskeleton in a control lily pollen tube. The cortical actin fringe is prominent in the apex. The shank contains longitudinally arranged actin filaments. Figure 2, B and C, show the actin cytoskeleton after 4 min of treatment with 2 nM Lat-B. The drug completely destroys the cortical actin fringe and disorganizes the microfilaments in the shank of the tube. Scale bar is 10 μm.

and C). In Figure 4B there are a few small fluctuations in both growth and Ca^{2+}, which show a close coordination. Finally after 20 min Lat-B treatment (Fig. 4C) both growth and Ca^{2+} exhibit a basal level, with growth at approximately 0.1 μm/s and Ca^{2+} at approximately 500 nM, and each one holding steady with only minor changes in value for at least 10 min.

Lat-B (2 nM) Causes the Alkaline Band to Move Apically

Repetitive measurements of the intracellular pH at 5-s intervals in cells loaded with 2′7′-bis-(2carboxyethyl)-5-(and-6)-carboxyfluorescein (BCECF)-dextran indicate that treatment with 2 nM Lat-B causes the acidic domain at the tip to disappear and the alkaline band to move closely to the extreme apex (Fig. 5). Unfortunately it has not been possible to conduct a reversal of this effect because the tubes rapidly burst after the removal of Lat-B, while in the presence of BCECF. The bursting of the recovering tubes appears to be peculiar to the presence of BCECF-dextran, because we do not observe this phenomenon in tubes recovering in the presence of fura-2-dextran (see Fig. 3).

Lat-B Increases the Level of G-Actin

Lat-B achieves its effect by binding to G-actin and preventing it from undergoing assembly into microfilaments (Spector et al., 1989). Therefore in the presence of Lat-B, the G-actin pool should increase. To test this prediction we have injected cells with fluorescently tagged DNase, which binds G-actin, and serves as a reporter for this form of actin. Because the binding of DNase to G-actin can itself retard actin polymerization and thereby affect pollen tube growth (Vidali et al., 2001), we have been careful to apply this reagent at levels that are sufficient to provide a good signal but too low to affect growth (Cárdenas et al., 2005; also see "Materials and Methods"). To gain semiquantitative data we have created a ratio-metric dye by mixing DNase Oregon green with tetramethyl-rhodamine-dextran.

Imaging DNase fluorescence in control cells reveals a relatively high level of G-actin in the apical domain (Fig. 6A), as shown previously (Cárdenas et al., 2005). When DNase-injected pollen tubes are treated with Lat-B (2 nM) the G-actin increases (Fig. 6, B and C). In Figure 6B, the differential interference contrast (DIC) paired image, which shows that the large organelles have invaded the clear zone, provides evidence that

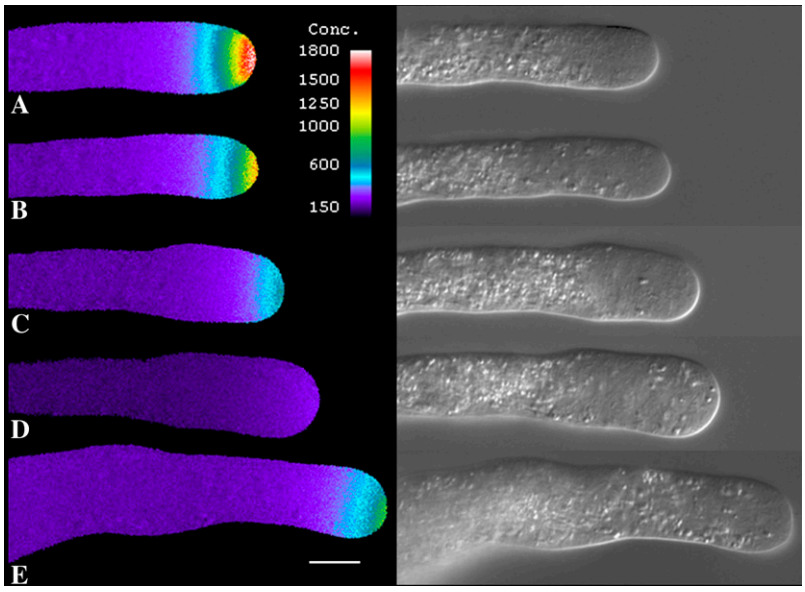

Figure 3. Visualization of intracellular Ca^{2+} following Lat-B treatment. A pollen tube loaded with fura-2-dextran shows a clear Ca^{2+} gradient (A). However, addition of Lat (2 nM) decreased the Ca^{2+} gradient slightly after 5 min (B), which became much more evident by 10 min (C). After 20 min the Ca^{2+} gradient has almost disappeared, and growth has stopped (D). Removal of Lat-B allowed recovery of growth and the tip-focused Ca^{2+} gradient, which became evident within 15 min (E). Scale bar is 10 μm.

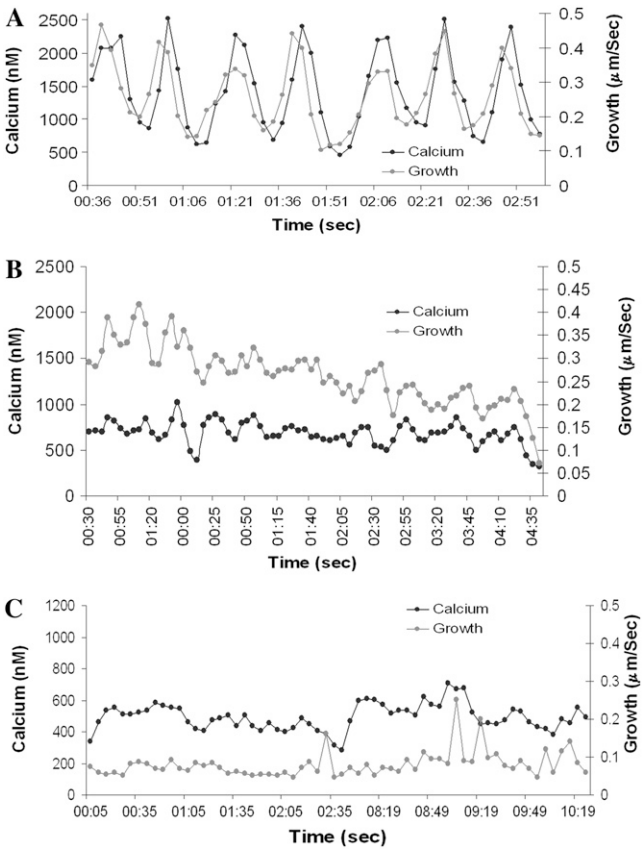

Figure 4. Graphical presentation of the effect of Lat-B on Ca^{2+}. Figure 4A provides a temporal trace of intracellular Ca^{2+} (black trace) and growth rate (gray trace) under control conditions. Both processes oscillate with the same periodicity, but not the same phase. Cross-correlation analysis indicates that Ca^{2+} follows growth. Figure 4B, which starts after 15 min of Lat-B exposure, shows that the drug induces a marked reduction in the growth rate and Ca^{2+} levels, and diminution in the oscillatory profiles of these processes. Figure 4C reveals that after 20 min in Lat-B the pollen tube exhibits a steady, but nonoscillating level of growth. Similarly, the Ca^{2+} concentration is reduced and nonoscillating.

Lat-B has exerted its effect on the pollen tube. The fluorescence image indicates that there has been a marked increase in G-actin, based on higher fluorescence ratio (Fig. 6B). At longer time intervals the continued presence of Lat-B causes the pollen tube to swell at the apex (Fig. 6C), within which the G-actin remains elevated, but especially so at the extreme apical end.

A further result that has emerged from this analysis is that the level of G-actin in the apex of control pollen tubes oscillates during growth. When the data are subjected to cross-correlation analysis, we find that the increase in G-actin follows the increase in growth rate by 91.3° (±2.3° SE, $n = 3$). A comparable analysis of the troughs reveals that they are nearly as strongly correlated with growth rate as are the peaks. But more importantly they are advanced over growth by an approximately equal interval of 84° (±2.8° SE, $n = 3$). A low level of G-actin, which we interpret as an increase in F-actin polymerization, thus anticipates the increase in growth rate.

DISCUSSION

The results presented expand our understanding of the role of actin polymerization in pollen tube growth. Although it has been known that Lat-B retards pollen tube growth, the use of flow-through chambers herein, reveals important details about the inhibitory process. In brief we find that Lat-B at 2 nM routinely requires 15 min or more before irregular growth oscillations are observed. Thereafter we reliably observe a decline in growth to a basal level (20–30 min), and finally after an additional 10 min to a nongrowing state. The results also show that the inhibitory effects of Lat-B on growth are closely coupled to a similar decline in the apical Ca^{2+} gradient. Thus oscillations in both growth and Ca^{2+} decline in parallel, and both reach nonoscillating states, which can persist for some minutes. Finally, when growth stops completely, the Ca^{2+} gradient disappears, and a basal level of the ion is observed throughout the length of the tube. Despite the severity of these effects, they are completely reversible when the tubes are returned to control culture conditions.

The cortical actin fringe, which is rapidly destroyed by Lat-B, emerges as a structure that plays a central role both in establishing cell/cytoplasmic polarity and in controlling rapid, oscillatory growth. In addition to the growth and Ca^{2+} effects noted above, Lat-B also produces an increase in G-actin, leads to a loss in the apical clear zone, and causes the alkaline band to move closely to the extreme apex of the cell. This last mentioned observation is particularly interesting because it suggests that there is a connection between the apical actin fringe, and the H^+-ATPase, which produces the alkaline band. It seems likely that the fringe controls the spatial location of the plasma membrane associated H^+-ATPase, and by extension the location of the

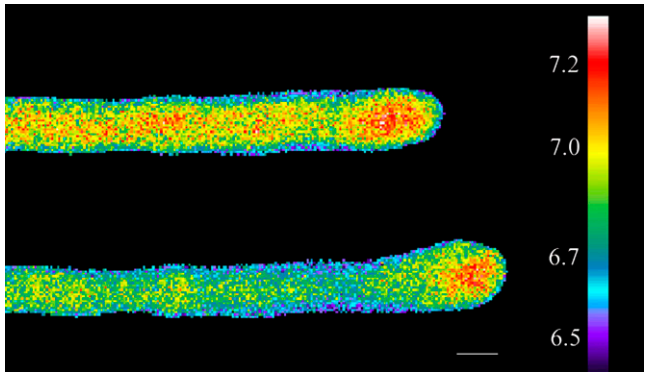

Figure 5. Lat-B causes the alkaline band to move forward into the apex of the pollen tube. The top shows a control lily pollen tube microinjected with BCECF-dextran, and the bottom shows the effect of Lat-B (2 nM) after 3 min. Scale bar is 10 μm.

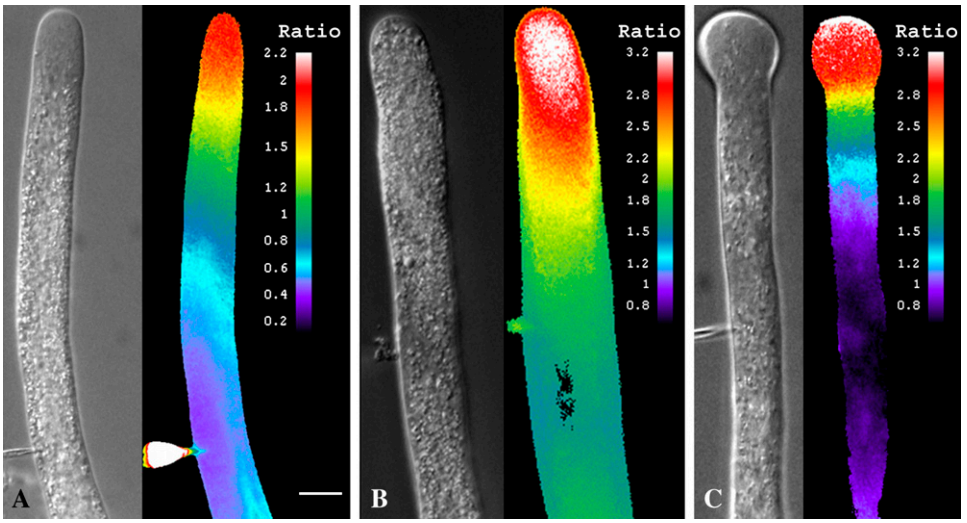

Figure 6. Effect of Lat-B on G-actin. Figure 6A shows a pollen tube that has been microinjected with DNase as a G-actin probe and tetramethyl-rhodamine-dextran as a reference marker for ratiometric measurements. The images indicate a pool of G-actin in the apical region of the tube. A corresponding DIC image reveals the morphology of the pollen tube. Figure 6B shows a pollen tube after 20 min in Lat-B. Note the increased fluorescent signal in the apex, and the complete disappearance of the clear zone in the DIC image. Figure 6C shows a pollen tube after 25 min in Lat-B. The fluorescent signal remains high in the swollen apex, but especially so toward the tip of the dome. Scale bar is 10 μm.

alkaline band as well as the pattern of extracellular proton currents, which seem pivotal in the regulation of pollen tube growth (Feijó et al., 1999; Lovy-Wheeler et al., 2006).

By what mechanism could the apical actin fringe promote oscillatory pollen tube growth? Pollen tube elongation, as in other plant cells, is assumed to be dependent on a balance between turgor pressure and a yielding of the cell wall (Cosgrove, 1993). Studies by Benkert et al. (1997) indicate that turgor pressure does not oscillate, and therefore we assume that the yielding properties of the cell wall are changing (Cosgrove, 1993). It is possible that the cortical actin fringe delivers vesicles to specific sites on the apical plasma membrane where the actin fringe terminates, which would define an annular shaped region at the cell surface. A targeted secretion could have the effect of locally weakening the cell wall and allowing turgor-driven cell expansion. In this regard it is pertinent that studies of root hairs, which like the pollen tubes grow by tip expansion, show that the region of maximal shape change at the cell surface is an annular ring, 2 μm to the outside of the polar axis (Shaw et al., 2000). In the pollen tube we suggest that when the fringe is destroyed with Lat-B, vesicles are no longer precisely targeted but randomly dock across the apical domain. Although new cell material may be inserted, it is not localized to specific regions and as a consequence does not modify the local cell wall yielding properties to the extent that can be achieved with focused secretion.

It is also possible that actin polymerization contributes directly to the driving force. There is a rich pool of G-actin in the apex of pollen tubes (Fig. 6; Cárdenas et al., 2005) and root hairs (He et al., 2006) where active

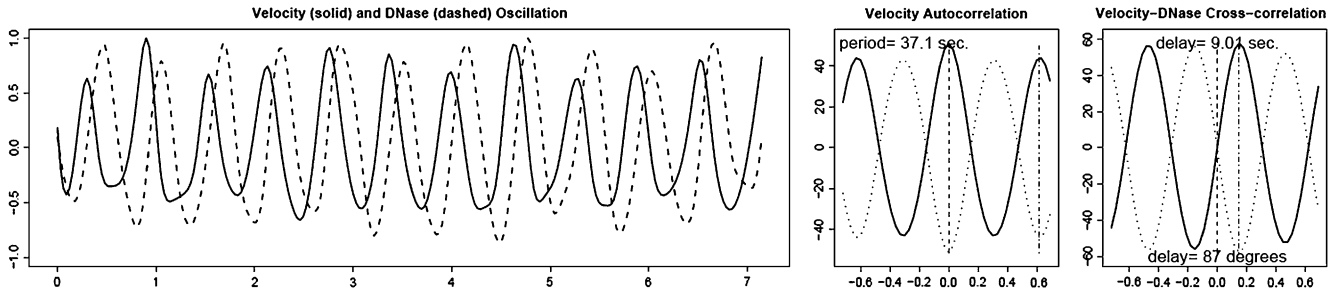

Figure 7. G-actin oscillations. Control cells were microinjected with the G-actin sensitive dye, DNaseI Oregon green, together with a reference dye, tetramethyl-rhodamine-dextran (70 kD). The graph shows that G-actin oscillates with the same period as the growth rate, but not with the same phase. The raw data, left, have been processed in "R" via a spline function to give additional resolution for the auto- and cross-correlation functions. Cross-correlation analysis indicates that the increase in G-actin follows the increase in growth velocity. In this example the period is 37.1 s, the G-actin peak is delayed 9.01 s, which equals an 87° phase delay, and the G-actin trough leads velocity by 9.0 s, which equals an 87° phase advance.

remodeling and polymerization occur. Moreover, it is well accepted in other systems such as the bacterium, *Listeria*, but also for inert beads and membrane vesicles that actin polymerization drives motility (Theriot, 2000; Carlier et al., 2003; Giardini et al., 2003; Mogilner and Oster, 2003). Quantitative measurements indicate that the maximum protrusive force produced would be a few (1–5 nN/μm^2; Upadhyaya et al., 2003; Footer et al., 2007). By extension to a pollen tube 16 μm in diameter, a cortical fringe, which occupies 25% of the total volume, would generate a maximum protrusive force of 50 to 250 nN. However, the pollen tube turgor pressure is 0.1 to 0.4 MPa (Benkert et al., 1997), which amounts to 20,000 to 80,000 nN per pollen tube. Given the magnitude of these turgor forces, it seems unlikely that actin polymerization contributes directly to the extension of the pollen tube, as has been similarly concluded for fungal hyphae (Money, 1997). We therefore favor the idea that the actin fringe transports vesicles to preferred sites on the plasma membrane, and that through focused secretion, the local cell wall properties are modified allowing turgor pressure to extend the apex.

The results showing that inhibition of actin polymerization with Lat-B causes the Ca^{2+} to decline stand at marked contrast with those of Wang et al. (2004) who report that application of CD or Lat-A to Arabidopsis pollen tubes or pollen grain protoplasts stimulates an increase in intracellular [Ca^{2+}]. They suggest that actin microfilaments regulate Ca^{2+} channels and that anti-actin agents, by degrading microfilaments, allow the channels to open and a Ca^{2+} influx (Wang et al., 2004). By contrast we find that Lat-B, which in action is very similar to Lat-A (Spector et al., 1989), causes a marked decline in intracellular Ca^{2+}. Moreover, the Ca^{2+} decline occurs in parallel with the Lat-B-dependent decrease in growth rate. These observations fit well with the idea that Ca^{2+} is regulated by growth, and not the reverse (Messerli et al., 2000), and that Ca^{2+} entry occurs through a growth-dependent stretch-activated channel (SACs; Dutta and Robinson, 2004). An explanation for the differences in the results between the studies of Wang et al. (2004) and ourselves is not known. However, some factors to consider include their use of 10 nM Lat-A versus 2 nM Lat-B herein. Also, their use of fluo-3-acetoxymethylester is a concern due to its tendency to sequester into intracellular compartments and obscure the cytosolic values of Ca^{2+} when compared to fura-2-dextran, which remains cytoplasmic. Further work may be needed, but at the moment we conclude that depolymerization of actin does not cause an increase in intracellular Ca^{2+}.

The studies with fluorescently tagged DNase indicate that Lat-B, as predicted, causes the G-actin pool to increase. A further observation reveals that this pool oscillates in control cells, with the increase in G-actin following, and the decrease in G-actin preceding the increase in growth rate. These results support the view that F-actin undergoes repetitive cycles of polymerization/depolymerization. Specifically F-actin appears to depolymerize following the peak in growth rate, and repolymerize in anticipation of the increase in growth rate. These conclusions are consistent with those showing that both the formation of F-actin (Fu et al., 2001) and myosin-dependent motion (Lovy-Wheeler et al., 2007) increase in anticipation of growth.

Whereas actin depolymerization does not appear to regulate Ca^{2+}, changes in the ion may exert a profound effect on actin organization. It has been known for over 20 years that elevated Ca^{2+} causes fragmentation of F-actin in lily pollen tubes (Kohno and Shimmen, 1987). Recent progress on actin regulation allows us to construct a model for Ca^{2+}/actin interaction and to order the underlying activities both spatially and temporally within the context of oscillatory pollen tube growth. Under normal growth conditions, both the increase in G-actin and intracellular Ca^{2+} follow the peak in growth rate, with Ca^{2+} (+38°; Messerli et al., 2000; also herein) preceding G-actin ($+90^0$). These observations suggest that Ca^{2+} may contribute to the depolymerization of F-actin. A plausible scheme emerges when we realize that Ca^{2+}-sensitive actin binding proteins occur commonly in plants in general (Hussey et al., 2006), and pollen tubes in particular (Yokota and Shimmen, 2006). For example, the villin/gelsolin family includes several members that modify actin in a Ca^{2+}-dependent manner. Two villins, P-135-ABP (Yokota et al., 2000; 2005) and P-115-ABP (Yokota et al., 2005), which contain six gelsolin repeats plus the characteristic villin headpiece, cross-link and stabilize actin bundles in low Ca^{2+}, but stimulate depolymerization in regions of elevated Ca^{2+}-calmodulin (Yokota et al., 2005). Three different gelsolins, including PrABP80 from *Papaver rhoeas* (Huang et al., 2004), LdABP41 from *Lilium davidii* (Fan et al., 2004), and ABP29 from *Lilium longiflorum* (Xiang et al., 2007), which are presumably splice variants of villin, actively fragment and depolymerize F-actin, and cap the plus ends, in regions of elevated Ca^{2+}. Yet another family of Ca^{2+}-responding, actin binding proteins includes profilin, which is abundant in pollen tubes (Vidali and Hepler, 1997; Gibbon et al., 1999; Snowman et al., 2002). Profilin binds G-actin and participates in the regulated polymerization from existing filament plus ends. However, in regions of elevated Ca^{2+} profilin sequesters G-actin and prevents its polymerization into F-actin (Kovar et al., 2000; Snowman et al., 2002). Taken together, it seems evident that Ca^{2+}, in the presence of villin/gelsolin, and profilin would degrade the existing F-actin and prevent the polymerization of new microfilaments.

Additional players involved in Ca^{2+} and actin interaction include the phosphoinositides (Žárský et al., 2006) and Rops, the small GTPases that control key events involved in pollen tube growth (Hwang and Yang, 2006). Briefly, phosphoinositide 4,5, bisphosphate (PIP_2; Kost et al., 1999; Dowd et al., 2006; Helling et al., 2006) localizes to the apical plasma membrane as does the enzyme phospholipase C (Dowd et al., 2006; Helling et al., 2006), which catalyzes the cleavage of PIP_2 to diacylglycerol and inositol 1,4,5 trisphosphate

(IP_3). PIP_2 binds different actin binding proteins, including villin/gelsolin, and profilin (Yin and Janmey, 2003). IP_3 stimulates the release of Ca^{2+} from internal stores, and consequently may modulate the apical gradient of the ion (Franklin-Tong et al., 1996; Malhó, 1998; Monteiro et al., 2005). It seems pertinent to consider these growth-associated factors with the Rops, with which they may closely interact (Kost et al., 1999). Thus Rop1 also localizes to the apical plasma membrane; in addition its activity oscillates during pollen tube growth (Hwang et al., 2005). Rop1 appears to operate downstream through two different ROP INTERACTING CRIB domain (RIC) proteins, RIC3 and RIC4, in which RIC4 modulates the actin cytoskeleton whereas RIC3 participates in Ca^{2+} regulation (Gu et al., 2005). These factors may counteract one another with RIC4 stimulating actin polymerization and dynamics, whereas RIC3 facilitates Ca^{2+} influx and triggers the depolymerization of actin.

Based on these lines of information we suggest the following scenario to explain the interactive roles of Ca^{2+} and actin in the apex during oscillatory pollen tube growth (Fig. 8). When growth accelerates, there is an increase in Ca^{2+} that follows the increase in growth rate. The ion influx might be controlled by the opening of SACs (Fig. 8; Dutta and Robinson, 2004), and/or through the action of a Rop/RIC3-dependent pathway (Gu et al., 2005). Elevated Ca^{2+} locally activates villin/gelsolin and profilin, with the level of these actin binding proteins being modulated in part through the cleavage of PIP_2 by phospholipase C, which is also Ca^{2+} sensitive (Dowd et al., 2006; Helling et al., 2006). Gelsolin fragments and depolymerizes existing F-actin, causing an increase in G-actin (Yokota and Shimmen, 2006), whereas profilin retards the polymerization of new microfilaments (Kovar et al., 2000). The combined effect of Ca^{2+} elevation and the stimulation of different actin binding proteins results in a down-regulation of the actin cytoskeleton, and all processes dependent thereon.

However, as pollen tube growth slows, there will be a reversal of the processes that retard growth (Fig. 8). Thus as growth declines during the oscillatory cycle, the SACs (Fig. 8) close, preventing Ca^{2+} entry; in addition the [Ca^{2+}] is reduced through sequestration by the ER, mitochondria, and the vacuole (Sze et al., 2006), and extrusion by plasma membrane Ca^{2+}-ATPases (e.g. ACA9; Schiøtt et al., 2004). These conditions reduce the activity of villin/gelsolin and profilin. Actin polymerization increases, perhaps being driven in part by Rop/RIC4 activity (Gu et al., 2005), and pollen tube growth will again be enhanced. Other factors that will also contribute to the overall regulation of oscillatory

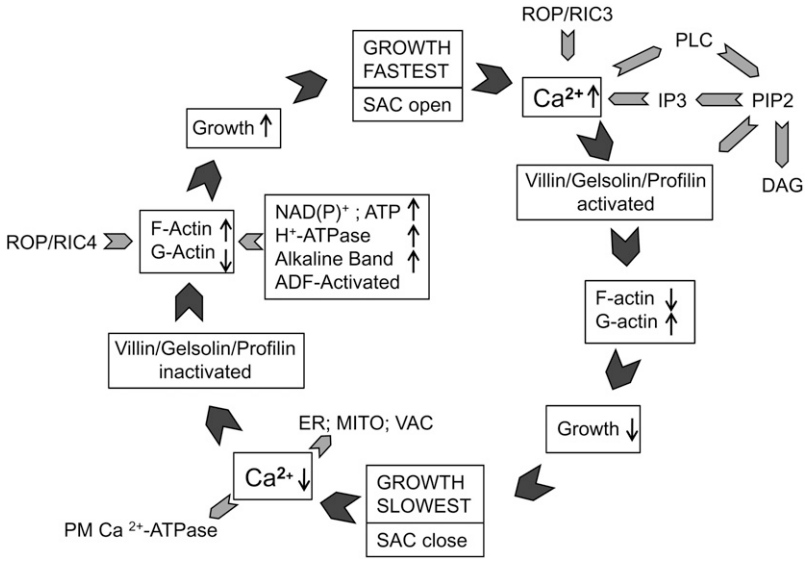

Figure 8. This diagram shows the temporal control of F-actin polymerization and emphasizes the role of Ca^{2+} and related factors. The circular pattern represents one complete cycle of an oscillation in growth rate. When growth is fast, SACs open allowing Ca^{2+} influx; the Rop/RIC3 signaling pathway may contribute to the Ca^{2+} increase. The Ca^{2+} rise activates different actin binding proteins (villin/gelsolin/profilin) both directly and indirectly through the stimulation of phospholipase C (PLC) and the degradation of PIP_2 to IP_3 and diacylglycerol (DAG). The formation of IP_3 might also contribute to the Ca^{2+} rise by releasing ions from internal stores. Combined, these processes cause F-actin depolymerization and a concomitant increase in G-actin. Growth slows, SACs close, and Ca^{2+} influx reduces. Ca^{2+} is also sequestered by intracellular compartments such as the ER, mitochondria (MITO), or the vacuole (VAC), and/or extruded to the outside by plasma membrane pumps. The reduced [Ca^{2+}] inactivates villin/gelsolin and profilin, allowing F-actin polymerization, with a decrease in G-actin. We suggest that metabolism, involving the oxidation of NADPH and an increase in ATP, enhances actin polymerization. An immediate effect would be to facilitate nucleotide exchange of ADP-G-actin. ATP will also activate the plasma membrane H^+-ATPase and increase the alkaline band, which in turn will activate ADF, which promotes actin turnover in regions of alkaline pH. The Rop/RIC4 signaling path may also contribute to actin polymerization. Together these processes enhance actin polymerization and stimulate pollen tube growth, possibly by targeting vesicles to selected sites at the cell surface.

growth and specifically to actin polymerization include the energy status and pH gradients. Recent work shows that NADPH oscillates with the oxidized form anticipating growth (Cárdenas et al., 2006). Here is it attractive to imagine that NADPH oxidation is synonymous with ATP production, which drives a host of essential processes, including the synthesis of cell wall components, membrane trafficking, Ca^{2+} and H^+ pumping, G-actin nucleotide exchange, and the formation of GTP needed to activate Rop (Cárdenas et al., 2006). Recent studies also show that the alkaline band in the clear zone increases in anticipation of growth acceleration, possibly due to an increase in ATP (Lovy-Wheeler et al., 2006). An elevated pH will stimulate ADF and promote actin turnover. Within this context the control of growth rate can be viewed as a balance between those conditions that promote actin polymerization, versus those that favor depolymerization. Actin polymerization stimulates growth, whereas Ca^{2+}, working through different actin binding proteins, serves as a brake, and limits the growth rate.

In conclusion, we have shown that preventing actin polymerization exerts a profound inhibitory effect on pollen tube growth. Lat-B at 2 nM markedly slows and even completely inhibits elongation. The underlying changes include a degradation of the apical actin fringe, a loss in cytoplasmic zonation, a diminution of the Ca^{2+} gradient, and a forward motion of the alkaline band. In considering the mechanism by which actin polymerization controls growth we favor the idea that the apical actin fringe targets vesicles to select regions in the apex, where exocytosis occurs. Through the targeted addition of material to the cell wall, loosening occurs that allows turgor-driven expansion. Our observations also suggest a close interaction between intracellular Ca^{2+} and the cytoskeleton in the pollen tube apex, wherein the ion, operating through different actin binding proteins, regulates the structure and activity of F-actin.

MATERIALS AND METHODS

Cell Culture

Lilium formosanum plants were first grown from seed in growth chambers for approximately 9 months to develop vigorous bulbs. The plants were then given a cold induction (approximately 5° C) for 6 weeks, which promotes flowering, and transferred to the greenhouse. Fresh pollen grains, harvested from flowering plants, were hydrated, germinated, and grown in pollen growth medium (PGM), which contained 15 mM MES, 1.6 mM H_3BO_3, 1 mM KCl, 0.1 mM $CaCl_2$, 7% Suc, and pH 5.5. After 30 min of germination and elongation on a rotary device at 25°C, the pollen tubes were allowed to settle for 5 min, and then 35 μL were mixed on a coverslip with an equal volume of 1.4% low melting point agarose (Type VII; Sigma-Aldrich) dissolved in PGM. After mixing, and wicking away the excess fluid, the preparation was chilled briefly (15 s) to gel the agarose. The pollen tubes were then allowed to recover for 15 min before examination with the microscope. To maximize the conditions and achieve optimal pollen tube growth, we set up a continuous perfusion system consisting of a peristaltic pump (Bio-Rad Laboratories), which can perfuse the PGM medium at a flow rate of 250 μL/s. This system also allowed us to administer the PGM with or without drugs, under conditions where there was minimal disturbance of pollen tube growth due to medium replacement. Those pollen tubes showing good growth rates and oscillations, and normal morphology were selected for further studies.

Microinjection of the Indicator Dyes

Pollen tubes were pressure injected with different probes as follows: fura-2-dextran (10 kD; 500 μM) for intracellular Ca^{2+}, BECEF-dextran (70 kD; 0.1 mg/mL) for pH, and DNaseI Oregon green (1.61 μM) for G-actin visualization. For microinjection the probes were centrifuged for 2 min at 7,000 rpm to remove nondissolved particles. Injection needles were pulled in a vertical pipette puller (model 700D; David Kopf Instruments) from borosilicate glass capillaries (World Precision Instruments). Using very thin-diameter plastic tubing attached to a micropipette, a small volume of injectate (0.5 μL) was introduced into the injection needle. The remaining volume of the needle was topped with distilled water. Following insertion of the needle into the pollen tube, approximately 100 μm from the tip, the desired probe was pressure injected into the pollen tube.

Live Cell Imaging: Determination of Ca^{2+}, pH, and G-actin

Pollen tube images were acquired using a CCD camera (Quantix Cool Snap HQ; Roper Scientific) attached to a Nikon TE300 inverted microscope (Nikon Instruments) with a 40×/1.3 numerical aperture oil immersion objective lens. All the equipment was operated with MetaMorph/MetaFluor software (Molecular Devices). Microinjected cells were excited using a xenon illumination source (DG-4; Sutter Instruments) that contains a 175-W ozone-free xenon lamp (330–700 nm) and a galvanometer for fast switching between excitation wavelengths. A filter wheel system (Lambda 10-2; Sutter Instruments), mounted immediately before the CCD camera, was used to control the position of emission filters for fluorescence ratio imaging, and a polarizing filter for Nomarski DIC imaging. The setup allowed fast (<1 s) acquisition of the ratio pair and the corresponding DIC image. The tracking function in MetaMorph was used to process the DIC images and calculate growth rate, amplitude, and frequency of the oscillations.

For Ca^{2+} determinations, fura-2 dextran loaded cells were excited at 340 and 380 nm, with excitation collected at 510 nm. Image pairs were also matched with a corresponding DIC image to show the status of the pollen tube. The two fluorescence images were ratioed to provide a quantitative map of the Ca^{2+} levels throughout the pollen tube. Ca^{2+} calibration was performed using buffer kit number two (Molecular Probes) and the kilodaltons calculated from the dissociation constant calculator Web site from Molecular Probes (http://www.probes.com).

For pH imaging, pollen tubes loaded with BCECF-dextran were excited at 440 and 495 nm, with emission at 535 nm. Although the amount of dye injected could not be tightly controlled, we attempted to work at levels below 1 μM, because it has been shown that higher concentrations dissipate local pH gradients (Feijó et al., 1999; Lovy-Wheeler et al., 2006). The total dye concentration in the cell was estimated by quantifying the fluorescence emission of the independent channel (440 nm) as described previously (Feijó et al., 1999). The application of 4 μL of dye on an 18-mm coverslip forms a 16-μM layer of dye, which roughly corresponds to the thickness of lily pollen tubes. The calibration curve assured us that we were working in the appropriate dye range. All filters were purchased from Chroma Technology. Images were binned (3 × 3) to improve the signal above background. In vitro calibrations were performed using 70-kD BCECF-dextran in a pseudocytosol medium (Poenie, 1990; Feijó et al., 1999) composed of 100 mM KCl, 30 mM NaCl, 500 mM mannitol, 40% Suc, 25 mM MES, and 25 mM HEPES adjusted to pH 6.3, 6.5, 6.7, 6.9, 7.1, 7.3, 7.5, and 7.8.

For G-actin imaging, DNaseI Oregon green was injected together with tetramethyl-rhodamine-dextran (70 kD), a reference marker. Because DNase can inhibit pollen tube growth by modulating actin polymerization, we therefore kept its final concentration between 0.15 and 0.2 μM, which is approximately 10-fold below that needed to cause half-maximal inhibition of elongation (1.9 μM; Vidali et al., 2001). Following injection, the cells were then excited at 484 nm (Oregon green) and 555 nm (tetramethyl-rhodamine), with emission being collected at 545 and 600 nm, respectively. Imaging was controlled with MetaMorph/MetaFluor. Finally the images were prepared for publication using Adobe Photoshop. Splining and auto- and cross-correlation analysis were carried out using the convolve function in an "R" computation environment (Maindonald and Braun, 2007).

Chemical Fixation

Pollen tubes were cultured 1 to 2 h, treated with 2 nM Lat-B for 4 min, and then were simultaneously fixed and permeabilized with a buffer composed of

100 mM PIPES (or 100 mM 3-{[2-hydroxy-1,1-bis(hydroxymethyl)ethyl]amino}-1- propanesulfonic acid [TAPS]), 5 mM $MgSO_4$, 0.5 mM $CaCl_2$, 0.05% Triton X-100, 5 mM ethylene glycol bis[sulfosuccinimidylsuccinate], 1.5% formaldehyde, and 0.05% glutaraldehyde at pH 9 for 0.5 to 1 h. The growth medium was completely removed before adding the fixative. The cells were rinsed free of fixative and then incubated in the same buffer as outlined above but at pH 7 and also containing 6.6 μM (10 μL/mL) Alexa 543-phalloidin (Molecular Probes) and 10 mM EGTA. Imaging, which began approximately 1 h after staining, was performed on a Zeiss LSM510 Meta confocal microscope using the HeNe 543-nm laser excitation, and a long-pass 568-nm emission filter.

Sequence data from this article can be found in the GenBank/EMBL data libraries under accession numbers

ACKNOWLEDGMENT

We thank our colleagues for many helpful discussions throughout the course of this investigation.

Received November 9, 2007; accepted February 4, 2008; published .

LITERATURE CITED

Benkert R, Obermeyer G, Bentrup FW (1997) The turgor pressure of growing lily pollen tubes. Protoplasma **198:** 1–8

Cárdenas L, Lovy-Wheeler A, Wilsen KL, Hepler PK (2005) Actin polymerization promotes the reversal of streaming in the apex of pollen tubes. Cell Motil Cytoskeleton **61:** 112–127

Cárdenas L, McKenna ST, Kunkel JG, Hepler PK (2006) NAD(P)H oscillates in pollen tubes and is correlated with tip growth. Plant Physiol **142:** 1460–1468

Carlier MF, Le Clainche C, Wiesner S, Pantaloni D (2003) Actin-based motility: from molecules to movement. Bioessays **25:** 336–345

Chen T, Teng N, Wu X, Wang Y, Tang W, Šamaj J, Baluška F, Lin J (2007) Disruption of actin filaments by latrunculin B affects cell wall construction in *Picea meyeri* pollen tube by disturbing vesicle trafficking. Plant Cell Physiol **48:** 19–30

Cosgrove DJ (1993) Wall extensibility: its nature, measurement and relationship to plant cell growth. New Phytol **124:** 1–23

Dowd PE, Coursol S, Skirpan AL, Kao T, Gilroy S (2006) Petunia phospholipase C1 is involved in pollen tube growth. Plant Cell **18:** 1438–1453

Dutta R, Robinson KR (2004) Identification and characterization of stretch-activated ion channels in pollen protoplasts. Plant Physiol **135:** 1398–1406

Fan X, Hou J, Chen X, Chaudhry F, Staiger C, Ren H (2004) Identification and characterization of a Ca^{2+}-dependent actin filament-severing protein from lily pollen. Plant Physiol **136:** 3979–3989

Feijó JA, Sainhas J, Hackett GR, Kunkel JG, Hepler PK (1999) Growing pollen tubes possess a constitutive alkaline band in the clear zone and a growth-dependent acidic tip. J Cell Biol **144:** 483–496

Footer MJ, Kerssemakers JW, Theriot JA, Dogterom M (2007) Direct measurement of force generation by actin filament polymerization using an optical trap. Proc Natl Acad Sci USA **104:** 2181–2186

Franklin-Tong VE, Drøbak BK, Allan AC, Watkins RAC, Trewavas AJ (1996) Growth of pollen tubes of *Papaver rhoeas* is regulated by a slow-moving calcium wave propagated by inositol 1,4,5-trisphosphate. Plant Cell **8:** 1305–1321

Fu Y, Wu G, Yang Z (2001) Rop GTPase-dependent dynamics of tip-localized F-actin controls tip growth in pollen tubes. J Cell Biol **152:** 1019–1032

Giardini PA, Fletcher DA, Theriot JA (2003) Compression forces generated by actin comet tails on lipid vesicles. Proc Natl Acad Sci USA **100:** 6493–6498

Gibbon BC, Kovar DR, Staiger CJ (1999) Latrunculin B has different effects on pollen germination and tube growth. Plant Cell **11:** 2349–2363

Gu Y, Dowd P, Li S, Vernoud V, Gilroy S, Yang Z (2005) A Rho family GTPase controls actin dynamics and tip growth via two counteracting downstream pathways in pollen tubes. J Cell Biol **169:** 127–138

He X, Liu YM, Wang W, Li Y (2006) Distribution of G-actin is related to root hair growth of wheat. Ann Bot (Lond) **98:** 49–55

Helling D, Possart A, Cottier S, Klahre U, Kost B (2006) Pollen tube tip growth depends on plasma membrane polarization mediated by tobacco PLC3 activity and endocytotic membrane recycling. Plant Cell **18:** 3519–3534

Hepler PK, Lovy-Wheeler A, McKenna ST, Kunkel JG (2006) Ions and pollen tube growth. Plant Cell Monographs **3:** 47–69

Hepler PK, Vidali L, Cheung AY (2001) Polarized cell growth in higher plants. Annu Rev Cell Dev Biol **17:** 159–187

Huang S, Blanchoin L, Chaudhry F, Franklin-Tong VE, Staiger CJ (2004) A gelsolin-like protein from *Papaver rhoeas* pollen (PrABP80) stimulates calcium-regulated severing and depolymerization of actin filaments. J Biol Chem **279:** 23364–23375

Hussey PJ, Ketelaar T, Deeks MJ (2006) Control of the actin cytoskeleton in plant cell growth. Annu Rev Plant Biol **57:** 109–125

Hwang JU, Gu Y, Lee YJ, Yang Z (2005) Oscillatory ROP GTPase activation leads the oscillatory polarized growth of pollen tubes. Mol Biol Cell **16:** 5385–5399

Hwang JU, Yang Z (2006) Small GTPases and spatiotemporal regulation of pollen tube growth. Plant Cell Monographs **3:** 95–116

Kohno T, Shimmen T (1987) Ca^{2+}-induced fragmentation of actin filaments in pollen tubes. Protoplasma **141:** 177–179

Kost B, Lemichez E, Spielhofer P, Hong Y, Tolias K, Carpenter C, Chua NH (1999) Rac homologues and compartmentalized phosphatidylinositol 4,5-bisphosphate act in a common pathway to regulate polar pollen tube growth. J Cell Biol **145:** 317–330

Kovar DR, Drøbak BK, Staiger CJ (2000) Maize profilin isoforms are functionally distinct. Plant Cell **12:** 583–598

Lovy-Wheeler A, Cárdenas L, Kunkel JG, Hepler PK (2007) Differential organelle movement on the actin cytoskeleton in lily pollen tubes. Cell Motil Cytoskeleton **64:** 217–232

Lovy-Wheeler A, Kunkel JG, Allwood EG, Hussey PJ, Hepler PK (2006) Oscillatory increases in alkalinity anticipate growth and may regulate actin dynamics in pollen tubes of lily. Plant Cell **18:** 2182–2193

Lovy-Wheeler A, Wilsen KL, Baskin TI, Hepler PK (2005) Enhanced fixation reveals the apical cortical fringe of actin filaments as a consistent feature of the pollen tube. Planta **221:** 95–104

Maindonald J, Braun WJ (2007) Data Analysis and Graphics Using R: An Example-Based Approach, Ed 2. Cambridge University Press, Cambridge, UK

Malhó R (1998) Role of 1,4,5-inositol triphosphate-induced Ca^{2+} release in pollen tube orientation. Sex Plant Reprod **11:** 231–235

Messerli MA, Creton R, Jaffe LF, Robinson KR (2000) Periodic increases in elongation rate precede increases in cytosolic Ca^{2+} during pollen tube growth. Dev Biol **222:** 84–98

Mogilner A, Oster G (2003) Force generation by actin polymerization II: the elastic ratchet and tethered filaments. Biophys J **84:** 1591–1605

Money NP (1997) Wishful thinking of turgor revisited: the mechanics of fungal growth. Fungal Genet Biol **21:** 173–187

Monteiro D, Liu Q, Lisboa S, Scherer GEF, Quader H, Malhó R (2005) Phosphoinositides and phosphatidic acid regulate pollen tube growth and reorientation through modulation of the $[Ca^{2+}]_c$ and membrane secretion. J Exp Bot **56:** 1665–1674

Poenie M (1990) Evidence for the alteration of intracellular fura-2 fluorescence ratios by viscosity and a simple correction. Cell Calcium **11:** 85–91

Schiøtt M, Romanowsky SM, Bækgaard L, Jakobsen MK, Palmgren MG, Harper JF (2004) A plant plasma membrane Ca^{2+} pump is required for normal pollen tube growth and fertilization. Proc Natl Acad Sci USA **101:** 9502–9507

Shaw SL, Dumais J, Long SR (2000) Cell surface expansion in polarly growing root hairs of *Medicago truncatula*. Plant Physiol **124:** 959–970

Snowman BN, Kovar DR, Shevchenko G, Franklin-Tong VE, Staiger CJ (2002) Signal-mediated depolymerization of actin in pollen during the self-incompatibility response. Plant Cell **14:** 2613–2626

Spector I, Shochet NR, Blasberger D, Kashman Y (1989) Latrunculins—novel marine macrolides that disrupt microfilament organization and affect cell growth: I. Comparison with cytochalasin D. Cell Motil Cytoskeleton **13:** 127–144

Sze H, Frietsch S, Li X, Bock KW, Harper JF (2006) Genomic and molecular analyses of transporters in the male gametophyte. Plant Cell Monographs **3:** 71–93

Theriot JA (2000) The polymerization motor. Traffic **1:** 19–28

Upadhyaya A, Chabot JR, Andreeva A, Samadani A, van Oudenaarden A (2003) Probing polymerization forces by using actin-propelled lipid vesicles. Proc Natl Acad Sci USA **100:** 4521–4526

Vidali L, Hepler PK (1997) Characterization and localization of profilin in pollen grains and tubes of *Lilium longiflorum*. Cell Motil Cytoskeleton **36:** 323–338

Vidali L, McKenna ST, Hepler PK (2001) Actin polymerization is necessary for pollen tube growth. Mol Biol Cell **12:** 2534–2545

Wang YF, Fan LM, Zhang WZ, Zhang W, Wu WH (2004) Ca^{2+}-permeable channels in the plasma membrane of Arabidopsis pollen are regulated by actin microfilaments. Plant Physiol **136:** 3892–3904

Xiang Y, Huang X, Wang T, Zhang Y, Liu Q, Hussey PJ, Ren H (2007) Actin binding protein 29 from *Lilium* pollen plays an important role in dynamic actin remodeling. Plant Cell **19:** 1930–1946

Yin HL, Janmey PA (2003) Phosphoinositide regulation of the actin cytoskeleton. Annu Rev Physiol **65:** 761–769

Yokota E, Muto S, Shimmen T (2000) Calcium-calmodulin suppresses the filamentous actin-binding activity of a 135-kilodalton actin-bundling protein isolated from lily pollen tubes. Plant Physiol **123:** 645–654

Yokota E, Shimmen T (2006) The actin cytoskeleton in pollen tubes: actin and actin binding proteins. Plant Cell Monographs **3:** 139–155

Yokota E, Tominaga M, Mabuchi I, Tsuji Y, Staiger CJ, Oiwa K, Shimmen T (2005) Plant villin, lily P-135-ABP, possesses G-actin binding activity and accelerates the polymerization and depolymerization of actin in a Ca^{2+}-sensitive manner. Plant Cell Physiol **46:** 1609–1703

Žárský V, Potocký M, Baluška F, Cvrčková F (2006) Lipid metabolism, compartmentalization and signaling in the regulation of pollen tube growth. Plant Cell Monographs **3:** 117–138